J. Mol. Biol. (1990) **214**, 811–817

Low Resolution Structure of Interleukin-1β in Solution Derived from ^{1}H–^{15}N Heteronuclear Three-dimensional Nuclear Magnetic Resonance Spectroscopy

G. Marius Clore[1], Paul C. Driscoll[1], Paul T. Wingfield[2] and Angela M. Gronenborn[1]

[1]*Laboratory of Chemical Physics, Building 2*
National Institute of Diabetes and Digestive and Kidney Diseases
National Institutes of Health, Bethesda, MD 20892, U.S.A.

[2]*Protein Expression Laboratory, Building 6B*
National Institutes of Health, Bethesda, MD 20892, U.S.A.

(Received 12 April 1990; accepted 27 April 1990)

A low resolution solution structure of the cytokine interleukin-1β, a 153 residue protein of molecular weight 17,400, has been determined on the basis of 446 nuclear Overhauser effect (NOE) derived approximate interproton distance restraints involving solely NH, $C^{\alpha}H$ and $C^{\beta}H$ protons, supplemented by 90 distance restraints for 45 hydrogen bonds, and 79 ϕ torsion angle restraints. With the exception of 27 $C^{\alpha}H$–$C^{\alpha}H$ NOEs, all the NOEs were assigned from a three-dimensional ^{1}H–^{1}H NOE ^{15}N–^{1}H heteronuclear multiple quantum coherence (HMQC) spectrum. The torsion angle restraints were obtained from accurate $^{3}J_{HN\alpha}$ coupling constants measured from a HMQC-J spectrum, while the hydrogen bonds were derived from a qualitative analysis of the NOE, coupling constant and amide exchange data. A total of 20 simulated annealing (SA) structures was computed using the hybrid distance geometry–dynamical simulated annealing method. The solution structure of IL-1β comprises 12 β-strands arranged in three pseudo-symmetrical topological units (each consisting of 5 anti-parallel β-strands), joined by turns, short loops and long loops. The core of the structure, which is made up of the 12 β-strands, together with the turns joining strands I and II, strands VIII and IX and strands X and XI, is well determined with a backbone atomic root-mean-square (r.m.s.) distribution about the mean co-ordinate positions of 1·2(±0·1) Å. The loop conformations, on the other hand, are poorly determined by the current data. A comparison of the core of the low resolution solution structure of IL-1β with that of the X-ray structure indicates that they are similar, with a backbone atomic r.m.s. difference of only 1·5 Å between the co-ordinates of the restrained minimized mean of the SA structures and the X-ray structure.

Interleukin-1β (IL-1β†) is a member of the cytokine family of proteins that play a central role in the immune and inflammatory responses. IL-1β is composed of 153 residues, has a molecular weight of 17,400, and possesses a wide range of specific biological activities that include, amongst others, stimulation of B-lymphocyte proliferation and fever induction (for reviews, see Dinarello, 1984, 1988; Oppenheim *et al.*, 1986; Moore, 1989). In two recent papers we presented the complete ^{1}H and ^{15}N assignment of the polypeptide backbone of IL-1β and the delineation of elements of regular secondary structure using principally three-dimensional (3D) ^{15}H–^{1}H heteronuclear nuclear magnetic resonance (n.m.r.) spectroscopy (Driscoll *et al.*, 1990*a*,*b*). We showed that IL-1β is composed of 12 β-strands, six of which form a β-barrel. In addition, we showed that IL-1β displays an internal 3-fold pseudo-symmetry comprising three topological units, each of which is made up of five anti-parallel β-strands. These results were in agreement with two high resolution X-ray studies (Finzel *et al.*, 1989; Priestle *et al.*, 1989) that were carried out independently and

† Abbreviations used: IL-1β, interleukin-1β; n.m.r., nuclear magnetic resonance; 3D etc., three-dimensional etc; NOE, nuclear Overhauser effect; NOESY, nuclear Overhauser enhancement spectroscopy; SA, simulated annealing; r.m.s. root-mean-square; HMQC, heteronuclear multiple quantum coherence; ^{1}H–^{15}N NOESY-HMQC, 3D ^{1}H–^{1}H-NOESY–^{15}H–^{1}H HMQC spectroscopy.

0022-2836/90/160811-07 $03.00/0

© 1990 Academic Press Limited

Table 1

Summary of NOE restraints used in structure calculations

	Sequential ($\|i-j\|=1$)	Medium range ($1<\|i-j\|\leq 5$)	Long range ($\|i-j\|>5$)
NH(i)–NH(j)	69	12	25
$C^{\alpha}H(i)$–NH(j)	142	23	56
$C^{\beta}H(i)$–NH(j)	88	4	0
$C^{\alpha}H(i)$–$C^{\alpha}H(j)$	0	2	25
Total	299	41	106

With the exception of the 27 $C^{\alpha}H$–$C^{\alpha}H$ NOEs that were assigned from a ^1H–^1H NOESY spectrum recorded in ^2H_2O, all the NOEs were derived from a 3D ^{15}N–^1H NOESY–HMQC spectrum recorded in H_2O. The NOESY mixing time used for the 2 experiments was 100 ms.

at approximately the same time as the n.m.r. analysis. In this paper we present the determination of a low resolution structure of IL-1β in solution on the basis of NOE derived approximate interproton distance restraints involving only the NH, $C^{\alpha}H$ and $C^{\beta}H$ protons. Thus, the structure is based on a very small subset of the total number of potentially assignable NOEs, and represents an initial structure that will be refined at a later stage after a larger number of restraints have been identified and extracted from a variety of heteronuclear 3D and 4D (Kay *et al.*, 1990) n.m.r. experiments. It nevertheless permits the delineation of the overall polypeptide fold, as well as an initial comparison between solution and X-ray structures.

All the NOEs were derived from a single 100 millisecond mixing time 3D ^{15}N–^1H NOESY–HMQC spectrum recorded on a 1·7 mM sample of uniformly ^{15}N-labeled IL-1β in 100 mM-sodium d_3-acetate (pH 5·4) and 95% H_2O/5% ^2H_2O at 36°C, with the exception of 27 $C^{\alpha}H$–$C^{\alpha}H$ NOEs that were assigned from a 2D ^1H–^1H NOESY spectrum recorded in ^2H_2O (with a 100 ms mixing time). Examples of the quality of the 3D data are provided by Driscoll *et al.* (1990*a*,*b*). The 446 NOEs used in the structure calculation comprised solely interresidue NH–NH, $C^{\alpha}H$–NH, $C^{\beta}H$–NH and $C^{\alpha}H$–$C^{\alpha}H$ NOEs, and a breakdown of these is presented in Table 1. The NOEs were classified into strong, medium and weak, corresponding to distance restraints of 1·8 to 2·7, 1·8 to 3·5 and 1·8 to 5·0 Å, respectively (1 Å = 0·1 nm). The NOE

Table 2

Structural statistics

	<SA>	$(\overline{SA})_r$
Deviations from expt		
Distance restraints (Å)		
All (536)	0·099 ± 0·019	0·070
Sequential ($\|i-j\|=1$) (299)	0·086 ± 0·014	0·076
Medium ($1<\|i-j\|\leq 5$) (41)	0·098 ± 0·043	0·131
Long ($\|i-j\|>5$) (106)	0·122 ± 0·055	0·029
H-bond (90)†	0·091 ± 0·044	0·035
Deviations from expt		
ϕ torsion angle restraints		
(deg.) (79)	1·2 ± 0·6	1·3
F_{NOE} (kcal mol^{-1})‡	276 ± 103	131
F_{ϕ} (kcal rad^{-1})‡	8·0 ± 8·7	8·4
F_{rep} (kcal mol^{-1})‡	68 ± 20	81
$E_{L\text{-}J}$ (kcal mol^{-1})§	−356 ± 20	−348
Deviations from idealized covalent geometry		
Bonds (Å) (2460)	0·006 ± 0·0006	0·006
Angles (deg.) (4462)	1·954 ± 0·010	2·406
Impropers (deg.) (929)‖	0·597 ± 0·039	0·611

The notation of the structures is as follows: <SA> are the 20 final dynamical SA structures; $\overline{SA}$ is the mean structure obtained by averaging the co-ordinates of the individual 20 SA structures best fitted to each other using residues comprising the 12 β-strands and the turns/loops connecting strands I and II, strands VIII and IX, and strands X and XI (i.e. residues 5 to 21, 25 to 31, 39 to 47, 56 to 63, 66 to 72, 78 to 85, 99 to 115, 120 to 136 and 140 to 150); $(\overline{SA})_r$ is the restrained minimized mean structure obtained by restrained minimization of the mean structure $\overline{SA}$. The number of terms for the various restraints is given in parentheses. The force constants for the covalent geometry terms are maintained at constant high values during the entire course of the dynamical SA calculations (600 kcal mol^{-1} Å^{-2} for the bond term and 500 kcal mol^{-1} rad^{-2} for the angular terms (1 cal = 4·184 J)). The simulated annealing protocol proceeds in 4 stages: (1) 200 cycles of Powell minimization with the force constant for the NOE (k_{NOE}) and ϕ torsion angle (k_{tor} restraints set to zero and the force constant k_{vdw} for the van der Waals' repulsion term set to 10^{-3} kcal mol^{-1} Å^{-4} (with the scale factor for the hard-sphere van der Waals' radius set to 1·0) to regularize the peptide bonds; (2) 3·75 ps of dynamics at 1000 K, during which time k_{vdw} is increased from 10^{-3} to 0·25 kcal mol^{-1} rad^{-4} by multiplying its value by 1·125 every 75 fs (with the van der Waals' radius scale factor set to 1·0), and k_{NOE} and k_{tor} are increased from 0·5 to 50 kcal mol^{-1} Å^{-2} and from 0·5 to 200 kcal mol^{-1} rad^{-2}, respectively, by doubling their values every 75 fs; (3) 1·5 ps of dynamics, during which time the temperature is reduced from 1000 K to 300 K in steps of 25 K every 50 fs; the values of k_{NOE} and k_{tor} are maintained at their values reached at the end of step (2), but the value of k_{vdw} is increased to 4 kcal mol^{-1} Å^{-4} and the van der Waals' radius scale factor is reduced to 0·8. The minor differences between this protocol and that published by Nilges *et al.* (1988) concern the lower starting value of k_{vdw} and the use of ϕ backbone torsion angle restraints in the present protocol. The final values of the force constants have been chosen empirically to ensure that the experimental restraints are satisfied within the errors of the data, the deviations from idealized covalent geometry are very small, and the non-bonded contacts are good (Nilges *et al.*, 1988).

† There are 2 distance restraints for every hydrogen bond identified on the basis of a qualitative interpretation of the NOE, coupling constant and amide exchange data: $r_{NH\text{-}O}$ = 1·8 to 2·3 Å and $r_{N\text{-}O}$ = 2·8 to 3·3 Å. A total of 45 hydrogen bonds were unambiguously identified in this manner (Driscoll *et al.*, 1990b).

‡ The values of the square-well NOE and torsion angle potentials (cf. eqns (2) and (3) of Clore *et al.* (1986)) are calculated with force constants (F) of 50 kcal mol^{-1} Å^{-2} and 200 kcal mol^{-1} rad^{-2}, respectively. The value of the quartic van der Waals' repulsion term (cf. eqn (5) of Nilges *et al.* (1988)) is calculated with a force constant of 4 kcal mol^{-1} Å^{-4}, with the hard sphere

van der Waals' radii set to 0·8 times the standard values used in the CHARMM empirical energy function (Brooks *et al.*, 1983).

§ $E_{L\text{-}J}$ is the Lennard-Jones van der Waals' energy calculated with the CHARMM empirical energy function (Brooks *et al.*, 1983). It is *not* included into the target function for simulated annealing.

‖ The improper torsion terms serve to maintain planarity and chirality; they also maintain the peptide bond of all residues in the *trans* conformation with the exception of the Tyr90–Pro91 peptide bond, which is maintained in the *cis* conformation on account of characteristic $C^{\alpha}H$–$C^{\alpha}H$ sequential NOEs and ^{13}C chemical shifts of the C^{β} and C$^{\gamma}$ atoms of Pro91 (G. M. Clore *et al.*, unpublished results).

Table 3

Backbone (N, C^{α}, C) atomic root-mean-square differences

	Backbone atomic r.m.s. difference (Å)	
	All residues (1–153)	Residues 5–21, 25–31, 39–47, 56–63, 66–72, 78–85, 99–115, 120–136 and 140–150†
<SA> *versus* $\overline{SA}$	1·99±0·23	1·19±0·12
<SA> *versus* $(\overline{SA})_r$	2·12±0·25	1·27±0·12
$(\overline{SA})_r$ *versus* $\overline{SA}$	0·75	0·43
<SA> *versus* X-ray	3·74±0·25	1·90±0·17
$\overline{SA}$ *versus* X-ray	3·17	1·50
$(\overline{SA})_r$ *versus* X-ray	3·27	1·48

The notation of the structures is given in Table 2, and "X-ray" is the refined 2 Å resolution crystal structure of Finzel *et al.* (1989).

† These residues represent the core of the molecule and comprise the 12 β-strands together with the turns joining strands I and II, strand VIII and IX, and strands X and XI.

restraints were supplemented by 90 restraints for 45 hydrogen bonds (r_{N-O} = 2·8 to 3·3 Å, r_{NH-O} = 1·8 to 2·3 Å) identified unambiguously on the basis of the NOE data involving the NH and $C^{\alpha}H$ protons, the $^3J_{HN\alpha}$ coupling constants and the NH exchange data (Driscoll *et al.*, 1990*b*). In addition to distance restraints, ϕ backbone torsion angle restraints derived from $^3J_{NH\alpha}$ coupling constants were also employed. Of the 111 $^3J_{NH\alpha}$ coupling constants (Driscoll *et al.*, 1990*b*) that could be measured from a ^1H–^{15}N HMQC-J spectrum (Kay & Bax, 1990; Forman-Kay *et al.*, 1990), 27 had values ≤6 Hz and 52≥8 Hz. The latter were converted to loose ϕ torsion angle restraints of −10° to −90° and −70° to −170°, respectively (Pardi *et al.*, 1984).

The structures were calculated using the hybrid distance geometry–dynamical simulated annealing (SA) method of Nilges *et al.* (1988). Briefly this involves two stages. In the first stage, a set of substructures comprising about a third of the total number of atoms is embedded from *n*-dimensional distance space into Cartesian co-ordinate space, without checking the triangle inequalities using the program DISGEO (Havel, 1986). These substructures are very crude but have approximately the correct polypeptide fold. The remaining atoms are then added, with the side-chains placed in an extended conformation, and the resulting structures are subjected to the protocol of dynamical SA described by Nilges *et al.* (1988), with a few minor modifications as described in the footnotes to Table 2, using the program XPLOR (Brünger, 1988). This particular protocol is designed to overcome large energy barriers along the path towards the global minimum region of the target function and during the early stages of the calculation permits chains to pass through one another. The target function that is being minimized comprises quadratic harmonic terms for bonds, angles and improper torsion angles (i.e. planes and chirality restraints), a quartic van der Waals' repulsion term, and quadratic square-well potential terms for the interproton distance and torsion angle restraints (Nilges *et al.*, 1988). It should be noted that *no* electrostatic, hydrogen bonding or 6–12 Lennard-Jones van der Waals' potential terms are used in the calculations. The total computational time required to compute each structure is partitioned into 3·5 hours for the initial substructure on a MicroVax 3500 workstation and 2·8 hours for the SA protocol on a Stellar GS 1000 workstation.

A total of 20 SA structures was computed, and the structural statistics and atomic r.m.s. differences are summarized in Tables 2 and 3, respectively. All the structures satisfy the restraints within the errors specified, exhibit very small deviations for idealized covalent geometry, and display good non-bonded contacts. The co-ordinates will be deposited in the Brookhaven Protein Data Bank. A best fit superposition of the 20 SA structures is shown in Figure 1. It is readily apparent from Figure 1(a) that, in general, the loops connecting the strands, as well as the N (residues 1 to 4) and C (residues 151 to 153) termini, are very poorly determined. This is a direct result of the complete absence of long-range NOE restraints for the loops. Indeed, all the long-range NOE restraints were those derived from the initial analysis of the regular secondary structure elements (Driscoll *et al.*, 1990*b*) and comprise $C^{\alpha}H$–$C^{\alpha}H$, $C^{\alpha}H$–NH and NH–NH NOEs across the sheets. The core of the structure, however, shown in Figure 1(b) and, comprising the 12 β-strands together with the turns connecting strands I and II, strands VIII and IX, and strands X and XI, is reasonably well determined, with a backbone atomic r.m.s. distribution about the mean co-ordinate positions of 1·2(±0·1) Å (Table 3). Indeed, this backbone atomic r.m.s. distribution is comparable to small protein structures (<100 residues) obtained without the use of stereospecific assignments (for reviews, see Wüthrich, 1986; Clore & Gronenborn, 1987, 1989). Thus, the present low resolution IL-1β structure is equivalent in quality to first-generation n.m.r. solution structures.

While the low resolution structure determination was in progress in our laboratory, the co-ordinates

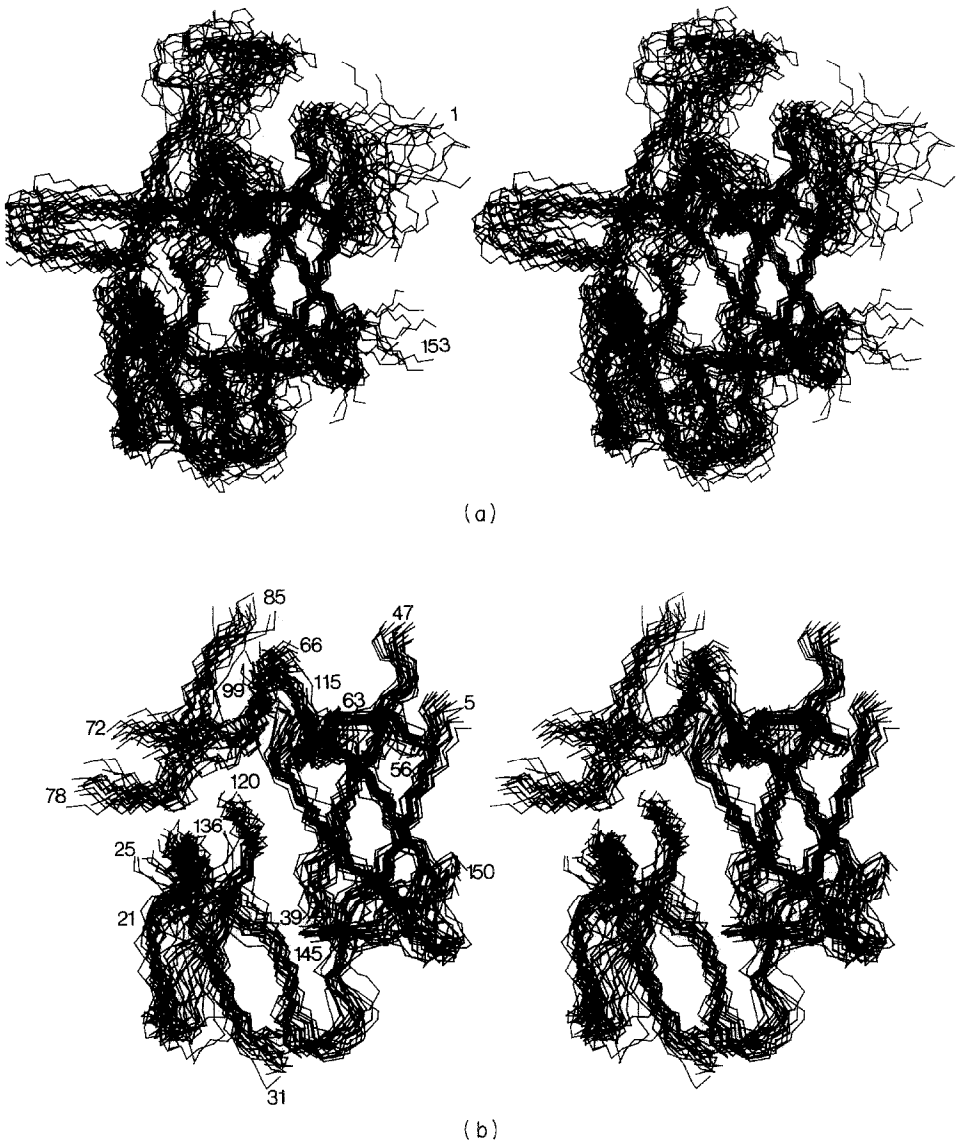

Figure 1. Best-fit superposition of the 20 SA structures of IL-1β for (a) all residues and (b) the core of the structure. The core comprises 12 β-strands, the turns connecting strands I and II, strands VIII and IX, and strands X and XI. Strand I is formed by residues 5 to 13, strand II by residues 15 to 21, strand III by residues 25 to 31, strand IV by residues 41 to 47, strand V by residues 56 to 63, strand VI by residues 66 to 72, strand VII by residues 78 to 85, strand VIII by residues 100 to 106, strand IX by residues 109 to 115, strands X by residues 120 to 125, strand XI by residues 130 to 136 and strand XII by residues 145 to 150. These strands are connecting by turns, short loops and long loops that make up the rest of the structure.

of the refined 2 Å resolution X-ray structure were kindly provided to us by Dr Barry Finzel. Figure 2 shows two views of a best-fit superposition of the restrained minimized average structure, $(\overline{SA})_r$, with the X-ray structure. It is clear that the agreement is respectable, with a backbone atomic r.m.s. difference of 1·5 Å. Both views clearly show that the β-barrel is made up of six anti-parallel β-strands in which strand XII (residues 145 to 150) is hydrogen bonded to strand I (residues 5 to 13), strand I to IV (residues 41 to 47), strand IV to V (residues 56 to 63), strand V to VIII (residues 100 to 106), strand VIII to IX (residues 109 to 115), and finally strand IX back to XII. The three topological units can also be discerned in the view shown in Figure 2(a) and (b). In particular, one topological unit is seen in the top half of the view and comprises strands IV, V, VI (residues 66 to 72), VII (residues 78 to 85) and VIII. The other two units are seen in the bottom half of the view, with the unit comprising strands VIII, IX, X (residues 120 to 125), XI (residues 130 to 136) and XII in front, and that comprising strands I, II (residues 15 to 21), III (residues 25 to 31), IV and XII behind.

It is interesting to note that the X-ray structure satisfies the interproton distance restraints approximately as well as the SA structures. One might therefore wonder why the backbone atomic r.m.s. difference for the IL-1β core between the X-ray structure and the mean SA structure (1·5 Å) is

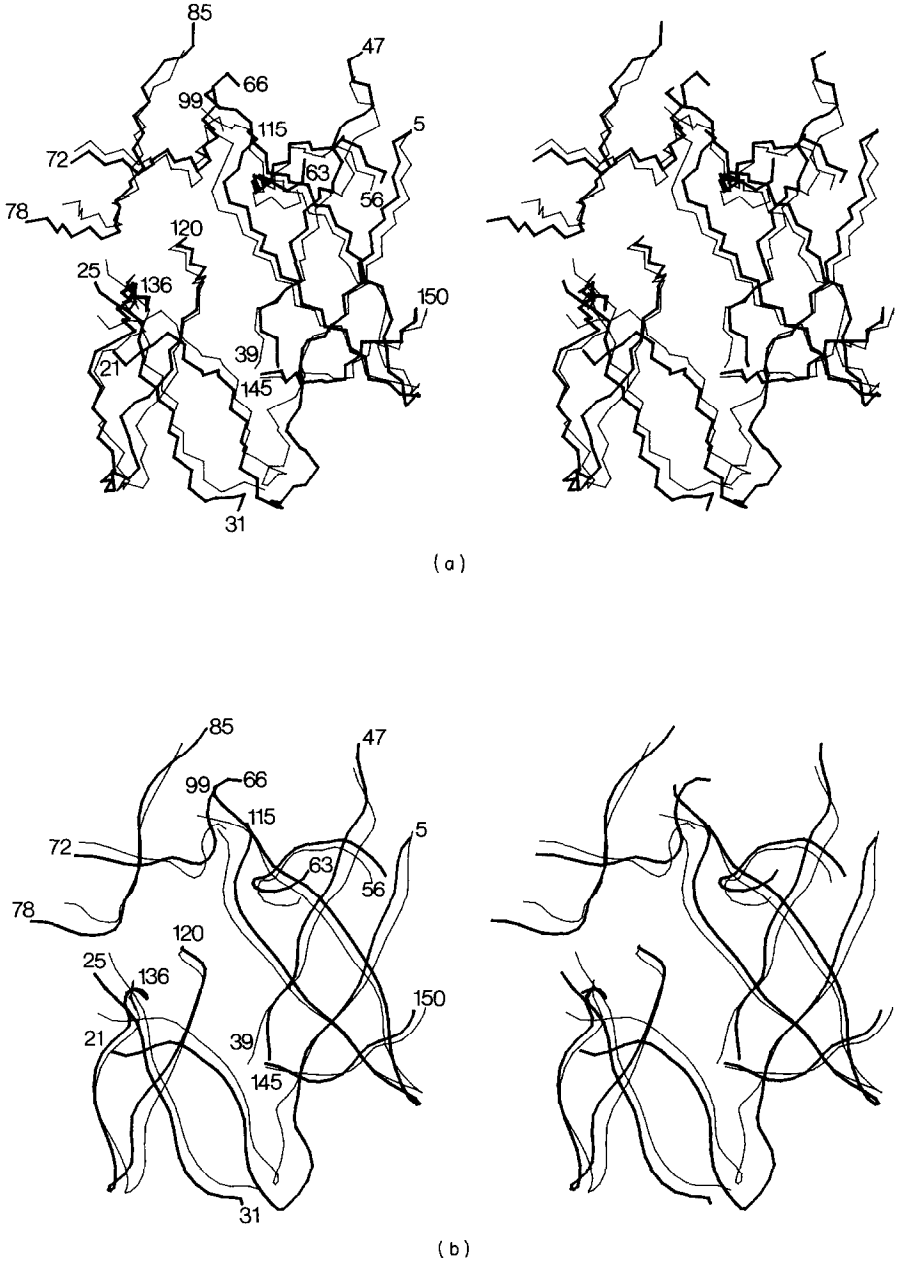

Fig. 2.

slightly larger than the backbone atomic r.m.s. distribution of the individual SA structures about the mean co-ordinate positions (1·2 Å). This difference does not reflect a genuine difference between the structure in solution and in the crystal, and the explanation for this phenomenon is subtle but obvious. In particular, the exact backbone conformation in the crystal structure depends on specific packing interactions, which are determined in turn by the interactions between individual side-chain conformations. The side-chain conformations in the SA structures, on the other hand, are essentially random, since the only interproton distance restraints employed in the calculations involve the NH, $C^{\alpha}H$ and $C^{\beta}H$ protons, and there are no side-chain restraints, other than those imposed by the van der Waals' repulsion term, which prevents atoms coming closer together than approximately the sum of their van der Waals' radii. Consequently, the probability of generating either an individual structure or an average structure identical with the X-ray structure is infinitessimally small.

Despite the fact that the current structure represents an initial low resolution structure of IL-1β in solution, the present study has a number of important implications. First, it shows that the algorithms employed for converting interproton distances into 3D structures are easily capable of handling proteins of around 150 residues, which is approximately 50% larger than any other protein structure determined by n.m.r. Second, it clearly demonstrates, at least in the case of β-sheet pro-

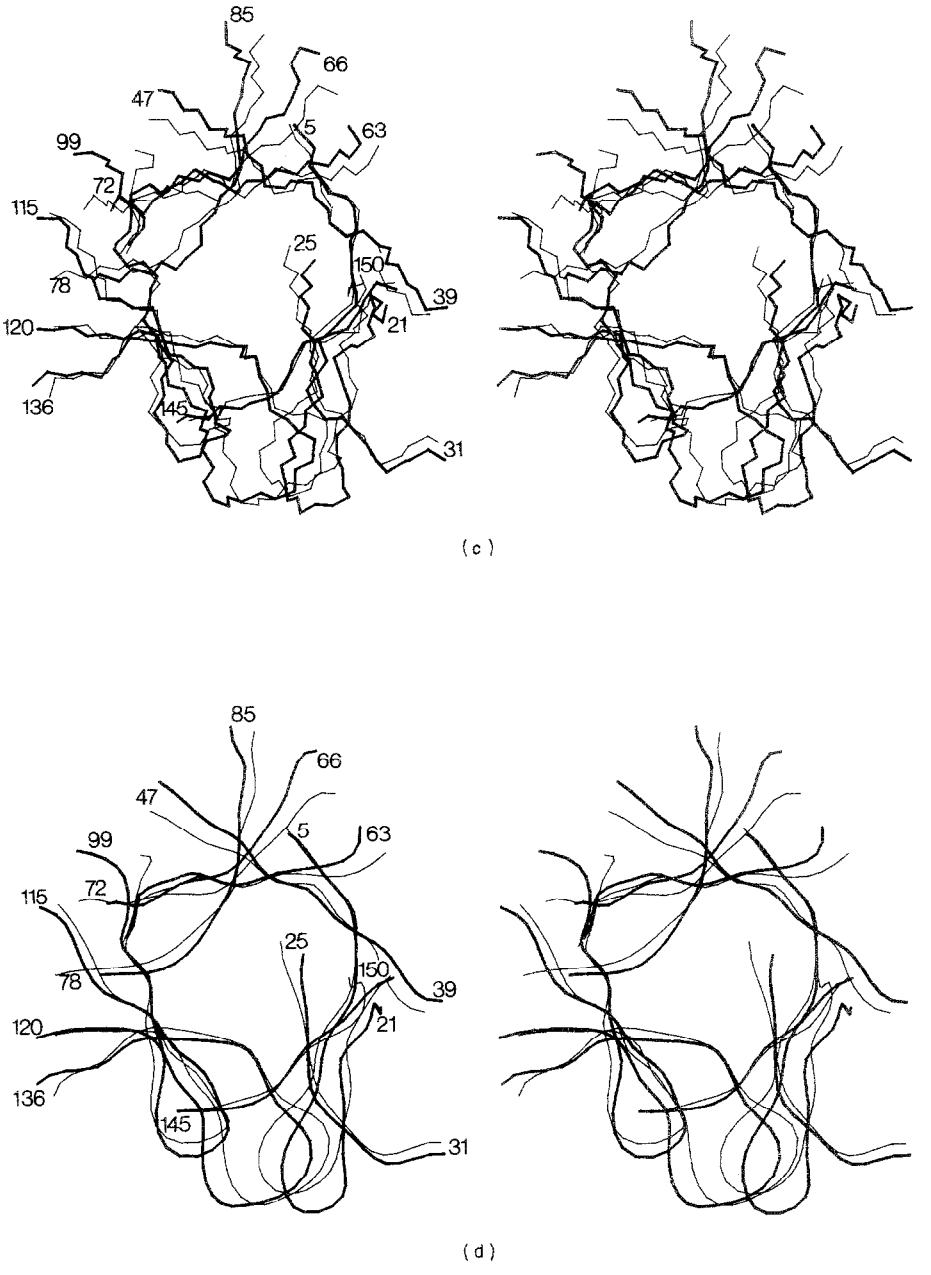

Figure 2. Two views showing a best-fit superposition of the restrained minimized average structure $(\bar{S}\bar{A})_r$ (thick lines) and the X-ray structure (thin line), for the core of the molecule comprising the 12 β-strands, and the turns connecting strands I and II, strands VIII and IX and strands X and XI. One view is displayed in (a) and (b), and another in (c) and (d). The N, C^{α} and C backbone atoms are shown in (a) and (c), while smoothed backbone representations are shown in (b) and (d) to help to guide the eye.

teins, that the global fold can be established with confidence on the basis of relatively few NOEs, and in particular of NOEs involving only the NH, $C^{\alpha}H$ and $C^{\beta}H$ protons. These NOEs are the easiest ones to assign and usually fall directly out of the sequential assignment procedure and secondary structure analysis. (In the case of α-helical proteins, it is clear that a few backbone–side-chain and/or side-chain–side-chain NOEs would also be required to determine the relative orientations of the helices.) Third, although the present structure is obviously of low resolution and contains no information whatsoever on the side-chain conformations, it is sufficient to delineate the polypeptide fold and to provide a basis for developing rational strategies involving, for example, site-directed mutagenesis to probe structure–function relationships and locate the active site (which in the case of IL-1β is still unknown). Thus, the structure not only establishes the 3D protein architecture, but also provides evidence to distinguish between those residues located at the surface from those within the interior of the protein, and reliably identifies loop regions from regions of regular secondary structure.

Naturally, we plan to extend the accuracy and precision of the solution structure of IL-1β. To this

end we have succeeded in obtaining complete ^{1}H and ^{13}C side-chain assignments by means of 3D ^{1}H–^{13}C–^{13}C–^{1}H correlation (*via* $^{1}J_{CC}$ couplings) and total correlation (with isotropic mixing of ^{13}C magnetization) experiments (Clore *et al.*, 1990). This will enable us to identify a large number of NOEs involving side-chains using a variety of 3D and 4D (Kay *et al.*, 1990) heteronuclear edited NOESY experiments, thereby permitting the determination of a high resolution structure of IL-1β in solution. Thus, it is hoped that complete high resolution solution structures of proteins up to M_r 20,000 will soon be within the reach of present n.m.r. technology.

We thank Dr Barry Finzel for the co-ordinates of the 2 Å resolution X-ray structure of IL-1β, and Dr Ad Bax for useful discussions.

References

Brooks, B. R., Bruccoleri, R. E., Olafson, B. D., States, D. J., Swaminathan, S. & Karplus, M. (1983). *J. Comput. Chem.* **4**, 187–217.

Brünger, A. T. (1988). *XPLOR Manual*, Yale University, New Haven, CT.

Clore, G. M. & Gronenborn, A. M. (1987). *Protein Eng.* **1**, 276–288.

Clore, G. M. & Gronenborn, A. M. (1989). *CRC Crit. Rev. Biochem. Mol. Biol.* **24**, 479–564.

Clore, G. M., Sukumaran, D. K., Brünger, A. T., Karplus, M. & Gronenborn, A. M. (1986). *EMBO J.* **5**, 2729–2735.

Clore, G. M., Bax, A., Driscoll, P. C., Wingfield, P. T. & Gronenborn, A. M. (1990). *Biochemistry*, in the press.

Dinarello, C. A. (1984). *Rev. Infect. Dis.* **6**, 51–95.

Dinarello, C. A. (1988). *Ann. N.Y. Acad. Sci.* **546**, 122–132.

Driscoll, P. C., Clore, G. M., Marion, D., Wingfield, P. T. & Gronenborn, A. M. (1990*a*). *Biochemistry*, **29**, 3542–3556.

Driscoll, P. C., Gronenborn, A. M., Wingfield, P. T. & Clore, G. M. (1990*b*). *Biochemistry*, **29**, 4668–4682.

Finzel, B. C., Clancy, L. L. Holland, D. R., Muchmore, S. W., Watenpaugh, K. D. & Einspahr, H. M. (1989). *J. Mol. Biol.* **209**, 779–791.

Forman-Kay, J. D., Gronenborn, A. M., Kay, L. E., Wingfield, P. T. & Clore, G. M. (1990). *Biochemistry*, **29**, 1566–1572.

Havel, T. F. (1986). *DISGEO*, Quantum Chemistry Program Exchange No. 507, Indiana University, Bloomington, IN.

Kay, L. E. & Bax, A. (1990). *J. Magn. Reson.* **86**, 110–126.

Kay, L. E., Clore, G. M., Bax A. & Gronenborn, A. M. (1990). *Science*, in the press.

Moore, M. A. S. (1989). *Immunol. Res.* **8**, 165 175.

Nilges, M., Clore, G. M. & Gronenborn, A. M. (1988). *FEBS Letters*, **229**, 317–324.

Oppenheim, J. J., Kovacs, E. J., Matsushima, K. & Durum, S. K. (1986). *Immunol. Today*, **7**, 45–56.

Pardi, A., Billetter, M. & Wüthrich, K. (1984). *J. Mol. Biol.* **180**, 741–751.

Priestle, J. P., Schär, H.-P. & Grütter, M. G. (1989). *Proc. Nat. Acad. Sci., U.S.A.* **86**, 9667–9671.

Wüthrich, K. (1986). *NMR of Proteins and Nucleic Acids*, Wiley, New York.

Edited by P. E. Wright